

Article

Effect of Hygrothermal Aging on Hydrophobic Treatments Applied to Building Exterior Claddings

Giovanni Borsoi ^{1,*}, Carlos Esteves ¹, Inês Flores-Colen ¹ and Rosário Veiga ²

¹ CERIS, Civil Engineering Research and Innovation for Sustainability, Instituto Superior Técnico, University of Lisbon, 1000-147 Lisbon, Portugal; carlosdcesteves@gmail.com (C.E.); ines.flores.colen@tecnico.ulisboa.pt (I.F.-C.)

² LNEC, National Laboratory for Civil Engineering, 1000-147 Lisbon, Portugal; rveiga@lnec.pt

* Correspondence: giovanni.borsoi@tecnico.ulisboa.pt; Tel.: +351-218-443-975

Received: 26 February 2020; Accepted: 3 April 2020; Published: 7 April 2020



Abstract: Hydrophobic materials are among the most commonly used coatings for building exterior cladding. In fact, these products are easily applied to an existing surface, significantly reduce water absorption and have a minimal impact on the aesthetic properties. On the other hand, although these products have a proven effectiveness, their long-term durability to weathering has not yet been systematically studied and completely understood. For these reasons, this study aims to correlate the effect of artificial aging on the moisture transport properties of hydrophobic treatments when applied on building exterior claddings. Three hydrophobic products (an SiO₂-TiO₂ nanostructured dispersion; a silane/oligomeric siloxane; and a siloxane) were applied on samples of limestone and of a cement-based mortar. The moisture transport properties (water absorption, drying, water vapor permeability) of untreated and treated specimens were characterized. Furthermore, the long-term durability of the specimens was evaluated by artificial aging, that is, hygrothermal cycles (freeze–thaw and hot–cold). All treatments have significant hydrophobic effectiveness and improve the long term-durability of the treated specimens. However, the results showed that the three hydrophobic products have different effectiveness and durability, with the SiO₂-TiO₂ nanostructured dispersion being the most durable treatment on limestone, and the siloxane the most suitable for cementitious mortar.

Keywords: hydrophobic products; silicon-based compounds; claddings; durability; moisture transport properties

1. Introduction

The use of coatings on building façades is a fundamental action for the protection of external surfaces from weathering. Protective coatings should be considered for the conservation of historical façades, as well as for the maintenance of modern buildings. In fact, these products can help in the conservation of ancient materials by increasing the durability of the treated surface.

Water is among the most aggressive atmospheric agents, being the main physical-chemical degradation cause of porous building materials [1]. In fact, water can trigger several surface anomalies both on ancient and modern buildings, leading to several physical (e.g., loss of cohesion and material, condensation in the interior of the building, reduction of thermal conductivity, formation of salt efflorescence, hygrothermal aging in buildings) and aesthetic changes (e.g., stains, biofilm formation) on the affected surface [1–3].

For these reasons, excessive water penetration and retention should be avoided in order to balance the water content in the façade cladding. In fact, porous building materials can balance the moisture content according to their water transport properties, that is, water vapor adsorption, water capillary

suction, and water vapor condensation [4,5]. Water transport mechanisms can act simultaneously, sequentially, or separately, and their action depends on the exposure conditions and on the moisture content of the material [6].

Through the formation of a thin protective coating, the application of hydrophobic treatments intends to reduce mostly water absorption, and thus, to protect the treated surface from the possible physical-chemical and biological alterations induced by the presence of water [7]. Additionally, surface coatings hinder the penetration of deleterious environmental particles (e.g., pollutants and salts) in the treated surface.

A wide majority of hydrophobic products present a surface tension lower than water and by modifying the contact angle of the treated surface help avoid wettability or limit water absorption within the surface [3,8,9]. In fact, hydrophobic products are generally non-polar materials, which repel water (which is polar), whereas they have an affinity with other non-polar materials, making them attractive to, for example, alkanes (fats and oils) and noble gasses [10].

Among the requirements of an ideal hydrophobic product, the protective coatings should be compatible with the treated material, and thus, not remarkably modify the physical-chemical properties of the treated surface. In fact, the hydrophobic materials should deeply penetrate the pore network and confer water-repellent properties to the treated material. However, they should not drastically alter the water vapor transport and the drying kinetics, and thus the breathability of the treated cladding [1,8].

The effectiveness of the hydrophobic products also depends on the chemical affinity between the product and the treated surface [11]. A lack of a proper knowledge of the hydrophobic products and of the moisture transport properties of the treated surface can lead to the formation of stains and byproducts (e.g., salts), alteration of the colour and brightness, and even an acceleration of the degradation of the treated surface. In addition to a proper hydrophobic effectiveness and compatibility with the treated surface, the hydrophobic product should have a suitable durability to weathering agents.

Organic silicon compounds, such as silanes, siloxanes, silicon resins and silicanates, are among the most commonly used hydrophobic products [12]. These materials have been widely used due to their high resistance to oxidation processes, UV radiation and extreme pH environment [13]. Additionally, these materials ensure ease of application and respect the aesthetic properties of the treated surface. When applied to the building material, the hydrolytically sensitive alkoxy groups of silicone compounds react with water or humidity, forming non-stable silanol intermediates, which spontaneously polycondensate to form stable covalent bonds. This hydrophobic film is irreversibly bonded to the mineral substrate [2,7].

Hydrophobic treatments are generally subjected to weathering and tend to alter their water-repellent properties (by physical-chemical degradation or leaching), and thus, protective action over time. The loss of hydro-repellency is attributed to the synergic effect of atmospheric agents (e.g., hygrothermal variations, solar radiation, rain, atmospheric pollutants) [1]. The accumulation of atmospheric particles with hydrophilic properties on the surface also has an important role in the surface degradation process [9,14]. Additionally, weathering can speed up the alteration and degradation of the polymeric structure of the hydrophobic material, inducing an increase of the polarity and a loss of water-repellency, as well as chromatic alteration and the formation of stains. In fact, photo-oxidation—induced by UV radiation and a degradation of the Si–O bonds due to the extreme pH environment—can lead to loss of adhesion, yellowing and a reduction of the surface gloss [8,9].

Although in some cases a long-term resistance of the hydrophobic treatment is reported [15], with an effective water repellence after 3–5 years of exposure to severe weathering [7,8], the durability of most commercially available hydrophobic products is not reported by manufacturers. Furthermore, the relationship between the physical-chemical properties of the hydrophobic product and of the treated material, and environmental factors, have not yet been completely understood.

For the reasons mentioned above, this paper aims to discuss the factors that influence the durability and effectiveness of hydrophobic products. Three commercially available products (a silicon and titanium dioxides-based nanostructured dispersion; a silane/ oligomeric siloxane; and a siloxane) were applied on limestone and on mortar specimens. The moisture transport properties (water absorption

by capillarity and under low pressure, drying, water vapor permeability) of untreated and treated samples were characterized. Furthermore, with the intention of evaluating the durability of these treatments to weathering, treated and untreated specimens were subjected to artificial aging tests, that is, hygrothermal cycles (freeze–thaw and hot–cold) and were then tested.

This work ultimately intends to provide tools to enhance the effectiveness and durability of hydrophobic products in the construction sector.

2. Materials and Methods

2.1. Materials

2.1.1. Substrates

Two types of substrates were selected for the application of hydrophobic products: (a) Moleanos limestone and (b) a cement-based rendering mortar.

Moleanos is a dense, fine-grained, yellowish bioclastic limestone (>98% CaCO₃, density = 2.67 g/cm³), quarried in central Portugal and used as a decorative flooring or finishing building material [16,17].

The rendering mortar was obtained by following the recommendation of the EN 1015-2 [18]. A pre-dosed cement-based mortar (weber.rev ip©) was used, by mixing three parts of pre-dosed mortar with one part of water (in volume); this was then applied on ceramic hollow bricks.

The characteristics of the limestone and of the mortar, as well as the substrate where the mortar was applied (ceramic brick), are presented in Table 1 [19]. Additionally, the cement-based rendering mortar has a higher surface roughness, if compared to the dense Moleanos limestone.

Table 1. Average results and standard deviation of capillary water absorption coefficient, open porosity and bulk density of the substrates [19].

Substrates	Capillary Absorption Coefficient (kg·m ⁻² ·min ^{-0.5})	Open Porosity (%)	Bulk Density (kg/m ³)
Limestone	0.252 ± 0.031	10.96 ± 1.31	2385 ± 34
Mortar	0.431 ± 0.018	30.23 ± 2.04	1441 ± 101
Ceramic brick	0.074 ± 0.031	25.49 ± 0.49	1979 ± 12

2.1.2. Hydrophobic Products

The selection of hydrophobic products was based on market research. The main aim was the evaluation of products with various chemical compositions and, therefore, that possibly differentiated in terms of their effectiveness and durability.

Three silicon-based products were chosen, selecting different manufacturers:

- H_{SILA/SIL}: A solvent-based silane/oligomeric siloxane-based emulsion, which also contains a biocide additive (≤ 0.01% in volume); the silane used is a triethoxyoctylsilane;
- H_{SIL}: A solvent-based siloxane product (polydimethylsiloxane);
- H_{NST}: A water emulsion of silicon (SiO₂) and titanium dioxides (TiO₂) nanoparticles, which contains a reduced concentration of silane (N-octyltriethoxysilane ≤ 2.5% in volume) and a biocide (≤ 0.0015% in volume).

Silane-modified siloxane polymers are widely adopted as hydrophobic materials; siloxane guarantees improved adhesion properties with the treated substrate, whereas the silane is used as coupling agent and improves the hydrophobic properties of the treatment [20].

Silica nanoparticles, which present hydrophilic properties, can be modified during their synthesis by adding a coupling agent such as silane or sodium sulphate, which confers hydrophobic properties and prevents nanoparticle agglomeration [21,22]. These products are generally composed of hydrophobic hybrid crystalline SiO₂–TiO₂ nanoparticles with a crystallite size equal to 5–20 nm [23,24].

The use in coatings of high refractive index oxides, such as TiO_2 , has significantly grown in recent years due to the advancements of nanoparticle manufacturing processes and because of their beneficial properties. Nanostructured titanium oxide has photocatalytic properties which can result in multifunctional self-cleaning and biocidal coatings [25].

The physical/chemical characteristics and application protocol of the hydrophobic products is reported in Table 2. It is worth noting that most solvent-based hydrophobic products can be harmful for both the operator and the environment, due to their high content of volatile organic compound (VOC) (e.g., polycyclic aromatic hydrocarbons and alkanes) [9]. Additionally, silane and biocide additives (isothiazol-3-one, 3-iodo-2-propynylbutyl carbamate, among others) are generally toxic for the operator and detrimental for the environment.

Table 2. Chemical and physical characteristics and amount of product used in the application of the hydrophobic products.

Hydrophobic Product	Color	Density * (g/cm^3) at $T = 20\text{ }^\circ\text{C}$ and $\text{RH}\% = 60$	Drying Time (h)**	Number of Applications	Amount of Product Per Application (L/m^2)
$\text{H}_{\text{SILA/SIL}}$	Whitish	1.02	24	2	1.01 ± 0.06
H_{SIL}	Transparent	0.78	2	1	0.40 ^(a)
H_{NST}	Whitish	1.01	3	2	0.11 ± 0.01

* As referred in the product technical sheet; ** Time necessary to achieve constant mass after the product application;

^(a) 1 application per specimen.

2.2. Methods

2.2.1. Specimen Preparation

Cylindrical specimens, with 20 cm diameter and 2 cm thickness, were drilled and cut from Moleanos limestone blocks and used for capillary water absorption, drying and water vapor permeability tests. Prismatic specimens (30 cm \times 30 cm, 2 cm thickness) were used for the analysis of water absorption under low pressure. Before the application of the hydrophobic product, in order to obtain a constant moisture content in all the specimens, limestone specimens were stored in a conditioned room at $T = 23 \pm 2\text{ }^\circ\text{C}$ and $\text{RH} = 50 \pm 5\%$.

Concerning the mortar specimens, cylindrical specimens with 20 cm diameter and 2 cm thickness were produced by using dedicated molds; these were used for water vapor permeability tests. Additionally, a 2 cm-thick layer of the mortar was applied on hollow ceramic bricks (29 cm \times 17 cm \times 4 cm). These latter specimens were used for all the other tests (capillary water absorption, drying kinetics and water absorption under low pressure).

All mortar specimens were cured for 2 days at $T = 23 \pm 2\text{ }^\circ\text{C}$ and $\text{RH} = 95 \pm 5\%$, and later stored in a conditioned room at $T = 23 \pm 2\text{ }^\circ\text{C}$ and $\text{RH} = 50 \pm 5\%$ for 26 days, before testing.

All specimens (limestone and mortar) were sealed along their side surface with liquid paraffin (applied multiple times by brushing, until obtaining a layer of approximately 1 mm).

2.2.2. Application Protocol

The three hydrophobic products were applied by brushing, following the recommendations of the products technical data sheets (Figure 1a). Two applications were carried (in orthogonal directions) in the case of $\text{H}_{\text{SILA/SIL}}$ and H_{NST} , whereas one application was performed in the case of H_{SIL} . The interval between applications was around 2 h for $\text{H}_{\text{SILA/SIL}}$ and 3 h for H_{NST} . The applications were performed under controlled conditions ($50 \pm 5\%$ RH, $T = 20 \pm 2\text{ }^\circ\text{C}$) and the treated specimens were stored at the same hygrothermal conditions for 7 days, with the aim of completing the polymerization of the silicon-based products. Untreated samples were stored in the same conditions.

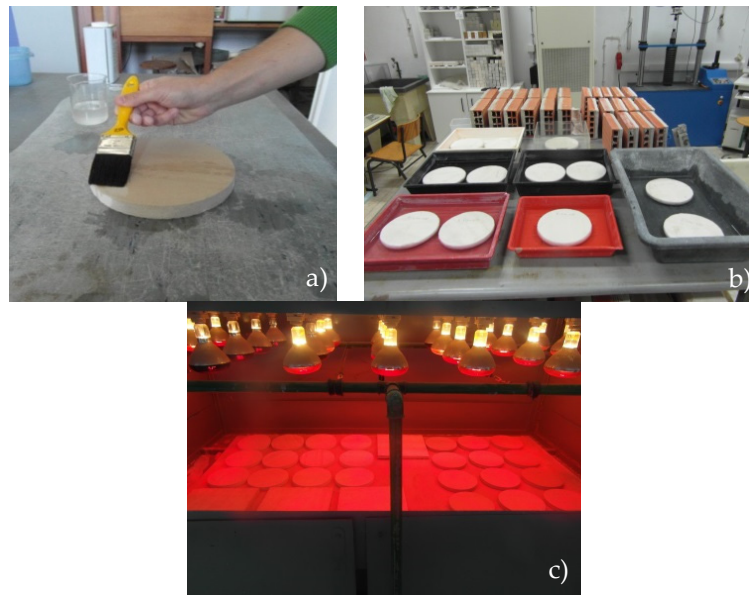


Figure 1. (a) Application of hydrophobic product on cylindrical limestone specimens; (b) capillarity water absorption on limestone and mortar specimens; (c) artificial aging test (hygrothermal cycles).

2.2.3. Moisture Transport Properties

The capillarity water absorption coefficient (C) was determined as the initial slope of the absorption curve using a protocol based on EN 1015-18 [26] (Figure 1b). The determination of water absorption by capillary action is achieved through the evolution of the amount of water absorbed by the solid unit surface area (kg/m^2), as a function of the square root of time ($t^{1/2}$).

Water absorption at low pressure was carried out with Karsten tubes applied on the specimens for 60 min, following RILEM recommendations [27]. The water absorption coefficient for 60 min (C^{60} , $\text{kg}\cdot\text{m}^{-2}\cdot\text{min}^{-1/2}$) was calculated according to the following Equation:

$$C^{60} = \frac{A_{bp} \times 10^{-3}}{A_c \times 10^{-4} \times \sqrt{60}} \quad (1)$$

where A_{bp} is the water mass absorbed after 60 min (kg), and A_c is the contact area of the pipe with the surface (assumed to be 5.7 cm^2 , i.e., the contact area of the Karsten pipe).

Drying tests were carried out sequentially at the end of the capillarity water absorption tests in order to allow a direct correlation between the water absorption and drying results. The drying kinetics of the specimens were verified according to RILEM [28] and UNI [29] recommendations, which considers the initial drying (based on the slope of the initial drying curve) and the drying index (DI). The latter is an empirical quantity that expresses the drying curve into a single quantitative parameter reflecting the global drying kinetics. The drying index, obtained from the average drying curve of those of the different specimens (in equivalent conditions), was calculated according to

$$DI = \frac{\int_{t_0}^{t_f} f\left(\frac{M_x - M_1}{M_1}\right) dt}{\left(\frac{M_3 - M_1}{M_1}\right) \times t_f} \quad (2)$$

where M_x is the specimen mass weighted during the drying process (g); M_1 is the specimen mass in dry state (g), M_3 the specimen mass in the saturated state (g), and t_f is the final time of the drying process (h).

Additionally, with the aim of understanding the influence of the hydrophobic products on the drying kinetics of the treated surface, the different steps of drying and the critical moisture content (i.e., the transition between the 1st and 2nd step of drying) were studied.

The water vapor permeability was determined as specified in EN1015-19 [30]. The water vapor diffusion resistance coefficient (μ) was calculated according to Equations (3) and (4):

$$\Lambda = \frac{m}{A \times \Delta p} \quad (3)$$

$$\mu = \frac{1.94 \times 10^{-10}}{\Lambda \times e} \quad (4)$$

where Λ is the water vapor permeance ($\text{kg/m}^2 \cdot \text{s} \cdot \text{Pa}$); m is the linear relationship slope of time versus mass change (kg/s); A is the specimen area (0.126 m^2); Δp is the difference between the outdoor and indoor vapor pressure (Pa); μ is the water vapor diffusion resistance coefficient; and e is the specimen thickness (m).

In all tests, three untreated specimens and nine treated specimens were analyzed, considering their average values and relative standard deviations.

2.2.4. Accelerated Aging Test

Accelerated aging tests were performed on untreated and treated limestone and mortar specimens to verify the durability of the hydrophobic treatments to weathering cycles [31]. Since temperature shock, rain and solar irradiation are the main degradation agents of porous materials [32], the specimens were subjected to hygrothermal cycles (hot–cold and freeze–thaw).

The test conditions, which represent extreme climate conditions, were adapted from EN 1015:21 [33]. This methodology was also validated in previous research by the authors [34,35]. Hot-cold cycles consist of storing the specimens firstly within a closed apparatus with infrared lamp (Figure 1c), which provides high temperature, and later within a deep-freeze cabinet with low temperature. Freeze-thaw cycles were carried out by exposing the specimens to a sprinkler system (simulating rain), followed again by a storage within a deep-freeze cabinet. Hot-cold and freeze-thaw cycles were carried out sequentially on the same specimens. Eight cycles of each type were performed, improving the indications (four cycles) of the norm previously mentioned (Figure 1c). Further details on the weathering cycles are provided in Table 3.

Table 3. Accelerated aging test: Hygrothermal cycles test conditions.

Hot-Cold Cycles	Freeze-Thaw Cycles	Exposure Time (h/mins)
Infrared lamps ($60 \pm 2 \text{ }^\circ\text{C}$)	Sprinkler system, water at $T = 20 \pm 1 \text{ }^\circ\text{C}$	$8 \text{ h} \pm 15 \text{ min}$
Stabilization ($20 \pm 2 \text{ }^\circ\text{C}$, $65 \pm 5\% \text{ RH}$)	Stabilization ($T = 20 \pm 2 \text{ }^\circ\text{C}$, $65 \pm 5\% \text{ RH}$)	$30 \pm 2 \text{ min}$
Deep freeze cabinet ($T = -15 \pm 1 \text{ }^\circ\text{C}$)	Deep freeze cabinet ($-15 \pm 1 \text{ }^\circ\text{C}$)	$15 \text{ h} \pm 15 \text{ min}$
Stabilization ($T = 20 \pm 2 \text{ }^\circ\text{C}$, $65 \pm 5\% \text{ RH}$)	Stabilization ($T = 20 \text{ }^\circ\text{C}$, $65\% \text{ RH}$)	$30 \pm 2 \text{ min}$

At the end of the hygrothermal cycles, specimens were stabilized for 48 h at $T = 20 \pm 2 \text{ }^\circ\text{C}$, $50 \pm 5\% \text{ RH}$. All the tests mentioned in the previous section were repeated on artificially aged untreated and treated specimens.

3. Results

3.1. Capillary Water Absorption and Water Absorption with Karsten Tubes

The results show that, in the case of limestone specimens, the capillary water absorption coefficient (C) of treated specimens considerably reduced after the application of the hydrophobic products (33% in the case of $\text{H}_{\text{Sila-Sil}}$, 51% with H_{sil} , 88% with H_{NST}) (Table 4, Figure 2).

Table 4. Average results and relative standard deviation of the capillarity water absorption coefficient (C) of treated and untreated specimens, before and after artificial aging tests.

Substrates	Capillarity Water Absorption Coefficient ($\text{kg}\cdot\text{m}^{-2}\cdot\text{min}^{-0.5}$)							
	Before Artificial Aging				After Artificial Aging			
	Untreated	Treated			Untreated	Treated		
		$\text{H}_{\text{Sila-Sil}}$	H_{Sil}	H_{NST}		$\text{H}_{\text{Sila-Sil}}$	H_{Sil}	H_{NST}
Stone	0.234 ± 0.031	0.175 ± 0.012	0.116 ± 0.032	0.040 ± 0.001	0.131 ± 0.031	0.053 ± 0.013	0.028 ± 0.010	0.068 ± 0.041
Mortar	0.182 ± 0.031	0.005 ± 0.001	0.004 ± 0.001	0.008 ± 0.001	0.124 ± 0.013	0.010 ± 0.001	0.011 ± 0.003	0.012 ± 0.002

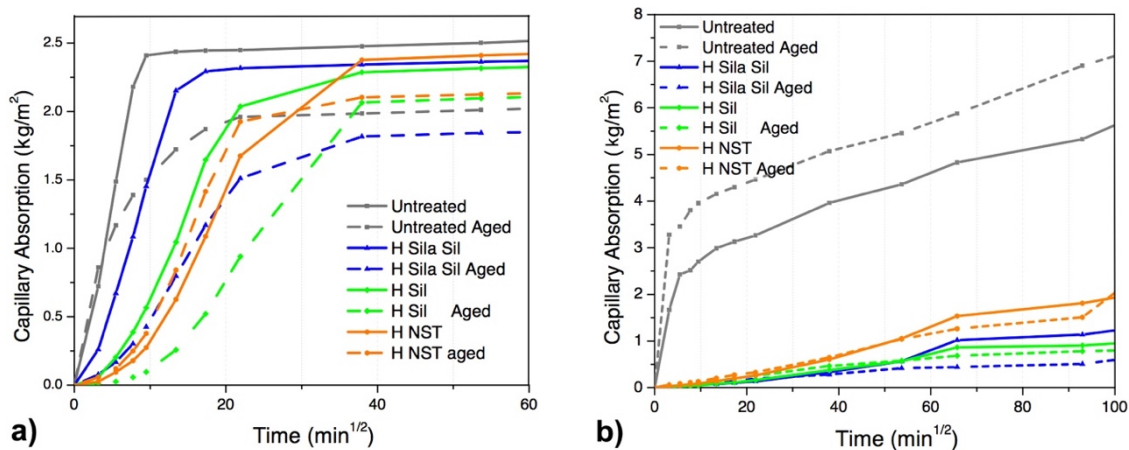


Figure 2. Capillary water absorption curves for the sound and treated substrates, before and after aging tests, of (a) limestone and (b) mortar, where solid lines are the unaged specimens, and dotted lines the aged specimens.

All hydrophobic products penetrated within the porous network of the substrate, reducing the wettability and providing a hydrophobic coating [9]. The higher reduction of the capillary water absorption coefficient of the specimens treated with H_{NST} , which can penetrate deeper within the treated substrate due to its nanosize [1], can be attributed to the chain arrangement (creation of Si-O-Ti bonds) of the TiO_2 - SiO_2 nanoparticles. The copolymerization of the TiO_2 and silane within the silica network can give rise to the formation of a homogeneous organic-inorganic hybrid xerogel, with improved hydrophobic properties [23,24].

After accelerated aging tests, untreated specimens show a significant reduction of the capillary water absorption (around 44%), which can be attributed to the modification (destruction) of capillary pores (typically observed in altered and decayed materials) [36]. In fact, a significant increase of porosity is observed mostly between 5 to 10 freeze-thaw cycles [37]. Thus, artificial aging induces the generation of new pores and the expansion of existing pores in the specimens.

Additionally, the specimens with H_{NST} treatment, which show the highest reduction of capillary water absorption before artificial aging, show an opposite trend after artificial aging, with a decrease of up to 60% when compared to the unaged specimens. On the other hand, aged specimens treated with $\text{H}_{\text{Sila/Sil}}$ and H_{Sil} show a significant reduction of the capillarity water absorption (80% and 50%, respectively), when compared to the untreated aged specimens.

This can be justified by the lower durability of H_{NST} treatment to hygrothermal aging cycles. As a matter of fact, it is reported [38] that weathering can induce a weakening of the film adhesion and reduce the durability of TiO_2 - SiO_2 protective coatings.

After aging, all specimens still maintain a significant reduction (40%, 21% and 52% for $\text{H}_{\text{Sila/Sil}}$, H_{Sil} and H_{NST} , respectively) of the capillary water absorption when compared to the untreated specimens.

Concerning mortar specimens, all treatments show a higher reduction of the capillarity water absorption when compared to treatments on limestone, although the total amount of absorbed water is

higher (total saturation of the specimens is not completely achieved at the end of the test). A remarkable reduction of the capillarity water absorption was observed in all treated mortar specimens (>95%), when compared to untreated specimens. This behavior is attributed to the higher open porosity of rendering mortars (Table 1), allowing the easier penetration of hydrophobic products into the pores of the substrate coating [19]. The deeper penetration of the hydrophobic products leads to a reduction of the wettability of the substrate, resulting in an almost hydrophobic surface. All treatments show a similar behavior, almost waterproofing the mortar specimens, and the treatments show a good durability after artificial aging, with a minimal increase of the capillarity water absorption coefficient when compared to unaged specimens.

Additionally, all aged treated mortar specimens significantly reduce their capillary water absorption coefficient when compared to aged untreated specimens. However, it is worth noting that a slight decrease of the capillarity water absorption coefficient was observed if comparing unaged treated specimens to aged treated ones. This modification can be attributed to the possible alteration of the pore size distribution of the substrates.

A possible cause for the reduction of capillary water absorption after freeze-thaw cycles can be the reduction of capillary suction, resulting from an increase in the amount of bigger pores (above the capillary range) as a consequence of micro-cracking. Additionally, in the case of the cement-based mortar, the exposure to water with these cycles can induce a self-healing effect that promotes hydration reactions, further explaining the reduction of the capillary absorption rate with ageing.

When considering the results of water absorption by Karsten tube in the limestone specimens, a trend similar to that seen in the capillarity water absorption test was observed (75% in the case of $H_{\text{SiLa-Sil}}$, 93% with H_{sil} , 92% with H_{NST}). In the case of the mortar specimens, the reduction was similar to that observed in capillarity water absorption tests (96% in the case of $H_{\text{SiLa-Sil}}$, 98% with H_{sil} , 99% with H_{NST}) (Table 5).

Table 5. Average results and relative standard deviation of the water absorption coefficient under pressure (C^{60}) of treated and untreated specimens, before and after artificial aging tests.

Substrates	Coefficient of Water Absorption at 60 min (C^{60}) ($\text{kg}\cdot\text{m}^{-2}\cdot\text{min}^{0.5}$)							
	Before Artificial Aging				After Artificial Aging			
	Untreated	Treated			Untreated	Treated		
		$H_{\text{SiLa-Sil}}$	H_{sil}	H_{NST}		$H_{\text{SiLa-Sil}}$	H_{sil}	H_{NST}
Stone	0.673 ± 0.178	0.167 ± 0.073	0.041 ± 0.022	0.053 ± 0.032	0.702 ± 0.131	0.083 ± 0.058	0.046 ± 0.021	0.147 ± 0.052
Mortar	0.893 ± 0.062	0.033 ± 0.012	0.023 ± 0.005	0.013 ± 0.005	0.906 ± 0.008	0.007 ± 0.009	0.013 ± 0.005	0.003 ± 0.002

If comparing the results of capillary water absorption and water absorption under low pressure of the untreated specimens, the opposite trend is seen. In fact, there is a reduction of capillary water absorption after aging; however, an increase of water absorption under low pressure is observed in equivalent conditions [39]. It is generally assumed that pores ranging from 1 to 10 μm act as capillary pores, whereas pores >10 μm contribute to the water permeability through gravity (e.g., percolation) or wind driven water ingress [40,41]. Thus, this confirms that artificial aging cycles possibly contribute to an increase in the amount of pores with dimensions greater than 10–20 μm .

Furthermore, $H_{\text{SiLa/Sil}}$ e H_{Sil} treatments decrease the water absorption coefficient under pressure after artificial aging, both when applied on mortar or limestone. On the other hand, a decrease of 25% in the C^{60} was observed in the aged limestone specimens treated with H_{NST} , if compared to the unaged specimens, whereas an opposite trend is observed when considering treated mortar specimens.

These results point out that $H_{\text{SiLa/Sil}}$ e H_{Sil} treatments have lower variation of the water absorption after artificial aging, compared to H_{NST} treatments. In fact, the latter shows both an increase of the capillary water absorption and water absorption under low pressure, possibly due to its physical-chemical alteration.

3.2. Drying Rate

When observing the drying curves, two stages can be observed (Figure 3). In the first stage of drying, called the constant drying period or initial drying rate, the drying front is at the surface and the drying rate is constant and controlled by the external conditions [42]. This first phase (initial drying rate) ends after 24 h in the case of all treated and untreated limestone and treated mortar specimens, whereas for untreated mortar specimens it ends after ≥ 72 h (Figure 3). When compared to the sound untreated specimens, all treated specimens decrease the initial drying rate products (first stage of drying), both in the limestone (3–12%) and mortar specimens (6–36%). More specifically, $H_{Si/la/Sil}$ has an almost negligible influence on the initial drying rate of the treated specimens (3% reduction, when compared to untreated specimens), whereas $H_{Si/la}$ and H_{NST} induce a slightly higher reduction (up to 12%).

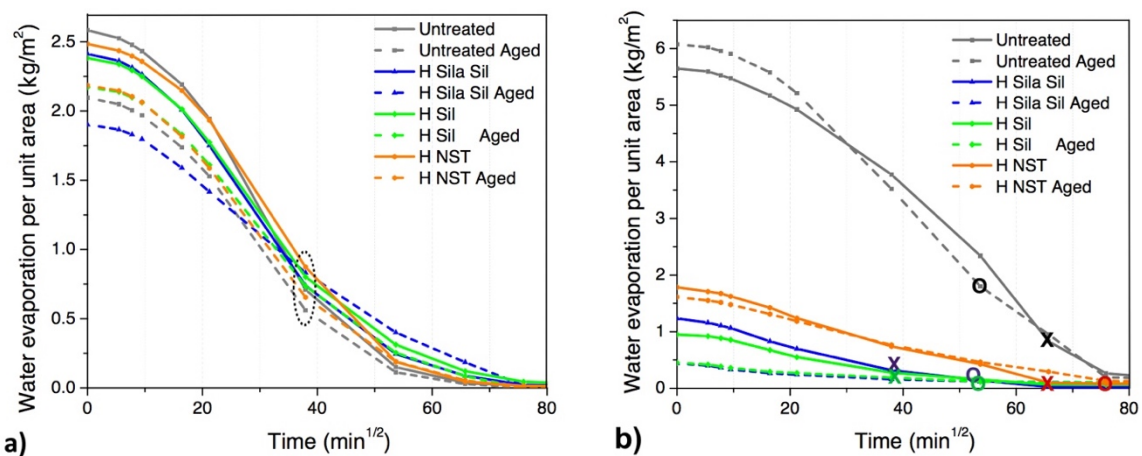


Figure 3. Drying curves for the sound, treated and aged substrate of (a) limestone and (b) mortar, where the dotted lines are the aged specimens, and solid lines the unaged specimens. The dotted ellipse (a) identifies the end of the 1st step of drying (critical moisture content) in (a), whereas this spot is highlighted as X (unaged specimens) or O (aged specimens) in (b).

In the second stage of drying, identified by the change in the slope of the drying curve, the moisture content can no longer support the demands of the evaporation flux, and, thus, the drying process occurs in the vapour phase. The transition between the first and second step of drying (i.e., the critical moisture content) occurs when the superficial moisture has evaporated. In this phase, the drying front progressively recedes into the material and the properties of the liquid and of the substrate control the rate of drying [42].

When considering the second stage of drying in limestone specimens, although the critical moisture content is identified at 24 h in all cases, it can be observed that (aged and unaged) untreated specimens almost achieve complete drying at 72 h, and a similar trend is observed in the case of the specimens treated with H_{NST} (Figure 3a). On the other hand, $H_{Si/la}$ and $H_{Si/la/Sil}$ slightly delay the drying process (the second step of drying ends at 96 h), when compared to H_{NST} treatment.

It can be concluded that the hydrophobic treatments induce only a slight retarding effect on the drying behavior of the limestone.

When considering the mortar specimens, all the hydrophobic treatments remarkably reduce the total amount of water absorbed; however, the H_{NST} treatment takes a longer time to dry completely when compared to the $H_{Si/la}$ and $H_{Si/la/Sil}$ treatments. Conversely, the H_{NST} treatment only slightly influences the initial drying rate (6% reduction) when compared to the $H_{Si/la/Sil}$ treatment (13%) and, especially, the $H_{Si/la}$ treatment (36%). Additionally, in accordance with the results observed in the previous section, H_{NST} treatment also increases the drying time (8%) in the mortar specimens, whereas $H_{Si/la}$ and $H_{Si/la/Sil}$ show a significant decrease (30–39%). The difference in the behavior of the

hydrophobic products is also observed in the second step of drying, which starts at 24 h in the case of H_{Sila/Sil} and H_{Sil} treatment, whereas the critical moisture content is identified at 72 h in the case of the H_{NST} treatment (as in the case of untreated specimens). Results obtained with contact angle measurements in a previous work confirm this trend and the drying index (Table 6), that is, a higher reduction of the wettability on both substrates in the case of H_{Sila/Sil} treatment [19].

Table 6. Drying index (I_s) of aged treated and untreated specimens, before and after artificial aging tests.

Substrates	Drying Index (DI)							
	Before Artificial Aging				After Artificial Aging			
	Untreated	Treated			Untreated	Treated		
		H _{Sila-Sil}	H _{Sil}	H _{NST}		H _{Sila-Sil}	H _{Sil}	H _{NST}
Stone	0.089	0.095	0.101	0.096	0.074	0.093	0.085	0.079
Mortar	0.191	0.117	0.133	0.207	0.215	0.171	0.159	0.155

After hygrothermal aging, H_{Sila/Sil} treatment show an improvement of the initial drying rate (20% and 27%, for limestone and mortar specimens, respectively), with worse results when compared to H_{NST} treatment (reduction of 5% and 24%, for limestone and mortar specimens, respectively) and H_{Sil} treatment (reduction of 9% and 12%, for limestone and mortar specimens, respectively). It can be seen that artificial aging slightly speeds up the drying process of the mortar specimens (the critical moisture content is identified at 48 h in the case of untreated aged specimens, and at 72 h with untreated unaged specimens). Additionally, in accordance with previous observations, the second step of drying of aged specimens treated with H_{Sil} and H_{Sila/Sil} starts at 48 h, and at 96 h in the case of the H_{NST} treatment (Figure 3b).

After artificial aging, H_{Sila/Sil} treatment shows the highest variation of drying behavior, with an increase (26%) of the DI for limestone and decrease of 21% for mortar specimens (the slower the drying, the higher the DI). In accordance with previous observations, H_{Sil} treatment also induces an increase (15%) of the DI for limestone, and, conversely, a significant decrease (26%) for mortar specimens. On the other hand, H_{NST} treatment shows the best performance on limestone specimens, with only a slight DI increase (6%), and, however, a significant decrease for mortar specimen (28%).

3.3. Water Vapor Permeability

The results of the water vapor permeability test, as expressed by the water vapor diffusion resistance coefficient (μ), show a μ decrease for all hydrophobic treatments on limestone and mortar specimens, reducing the breathability of the substrates (Table 7). The reduction in water vapor permeability is an inevitable consequence of the water repellence properties of polymer film; however, the lowest possible decrease is pursued [43].

Table 7. Average results and relative standard deviation of the water vapor diffusion resistance coefficient (μ) of treated and untreated specimens, before and after artificial aging tests.

Substrates	Water Vapor Diffusion Resistance Coefficient (μ)							
	Before Artificial Aging				After Artificial Aging			
	Untreated	Treated			Untreated	Treated		
		H _{Sila-Sil}	H _{Sil}	H _{NST}		H _{Sila-Sil}	H _{Sil}	H _{NST}
Stone	3.20 ± 0.31	10.46 ± 1.24	7.30 ± 1.34	5.57 ± 0.75	4.37 ± 1.17	12.58 ± 0.92	6.39 ± 0.90	4.67 ± 0.52
Mortar	2.19 ± 0.05	2.15 ± 0.05	2.27 ± 0.05	2.26 ± 0.14	2.75 ± 0.07	3.02 ± 0.07	2.69 ± 0.04	2.71 ± 0.14

This reduction is more significant in limestone specimens, whereas it is almost negligible in mortar specimens. In fact, an increase of μ of 227% (H_{Sila/Sil}), 129% (H_{Sil}) and 74% (H_{NST}) is observed on

treated limestone specimens, when compared to untreated ones, whereas a minimal μ increase (<4%) is observed on the treated mortar specimens.

After artificial aging, only the H_{NST} treatment applied on limestone maintains reasonably higher μ values (increase of 7%) when compared to untreated specimens, whereas H_{Sil} and $H_{Sila/Sil}$ treatments still induce a drastic μ increase (46% and 188%, respectively). In the case of mortar specimens, the higher increase of μ was observed with $H_{Sila/Sil}$ treatment (9%), and only a slight μ decrease in the case of H_{Sil} and H_{NST} treatments (<2%). In general, the hydrophobic treatment that illustrates the most suitable behavior to water vapor permeability was H_{NST} , with a moderate reduction of the μ on both substrates, even after artificial aging.

4. Discussion

The variation of the moisture transport properties of the substrates treated with the hydrophobic products is presented in Figure 4. In general, it can be observed that the hydrophobic products induce a decrease of the capillary water absorption coefficient (C), this decrease being more relevant with H_{NST} treatment on limestone specimens. However, after artificial aging, $H_{Sila/Sil}$ and H_{Sil} treatments show a higher durability, with a higher decrease of the C, if compared to specimens treated with H_{NST} . Concerning mortar specimens, all treatments maintain a similar water absorption coefficient (considerably lower than untreated specimens), even after artificial aging.

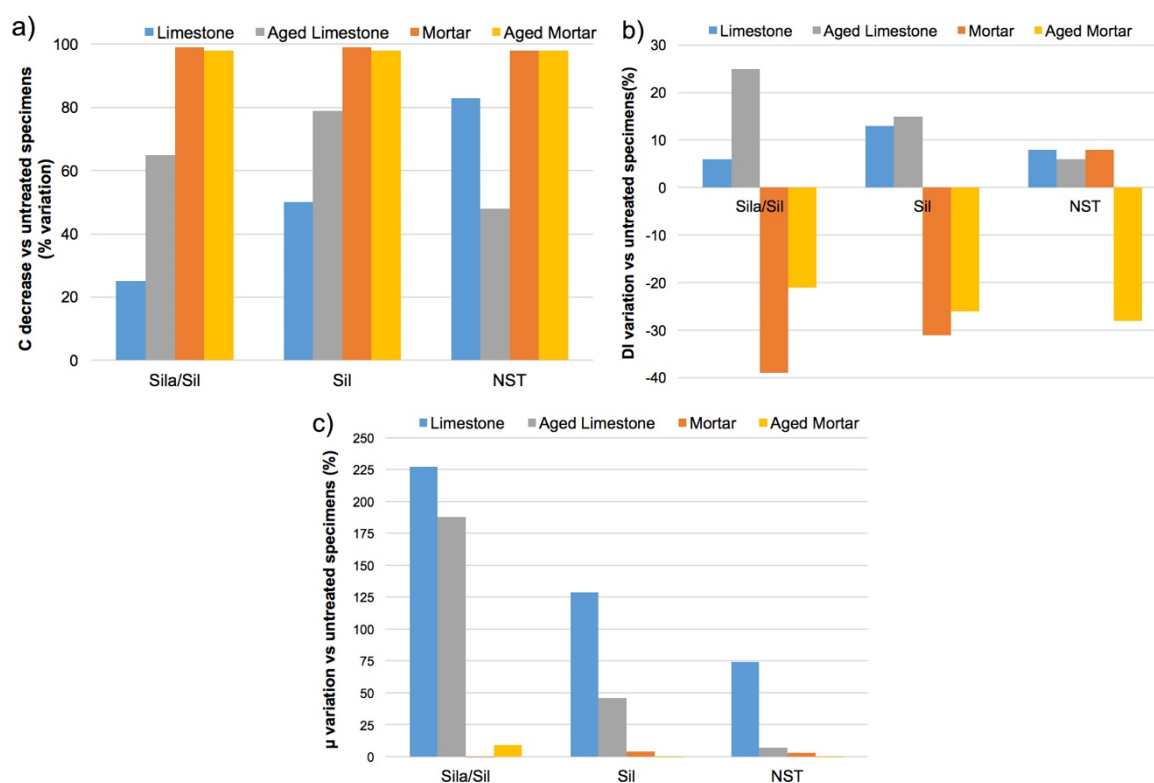


Figure 4. Percentage variation of (a) capillary water absorption coefficient (C), (b) drying index (DI) and (c) diffusion resistance of the water vapor coefficient (μ) of treated specimens, before and after artificial aging, when compared to untreated specimens.

The different moisture transport properties of mortar and limestone can be attributed to the higher open porosity (30%) of the mortar when compared to the studied limestone (11%). Additionally, mortar specimens generally have a higher volume of coarse pores (>100 μm) when compared to this type of compact Moleanos limestone [40].

Regarding the difference in the effectiveness and durability of the hydrophobic products, it is worth noting that (monomer) silane molecules are considerably smaller (10 to 15 \AA) when

compared to (oligomeric) siloxane molecules (25 to 75 Å) [44]. Thus, the longer Si–O chains of the siloxanes compared to the silane ones have a lower penetration depth in the compact limestone. Additionally, organo-modified siloxanes have an extremely high reactivity, which can hinder their in-depth penetration [2]. The silane has a potentially deeper penetration in the treated surface, with a higher reduction of the hydrophilicity and, thus, improved hydrophobic effectiveness. Furthermore, concerning the silane, it is generally assumed that the larger the molecule of the alkyl group linked to the silicon atom (which constitutes the structure of this compound), the higher the water repellency of the silane [8,45]. On the other hand, the long siloxane chains are more affected by environmental agents and weathering, undergoing degradation processes which can reduce their effectiveness as hydrophobic products [14].

The optimal performance obtained with the nanostructured product based on SiO₂ and TiO₂ (H_{NST}) on the limestone can probably be attributed to the chain arrangement of the TiO₂-SiO₂ nanoparticles, due to the creation of the Si–O–Ti bond [23]. In fact, the copolymerization of the TiO₂ and silane within the silica network can give rise to the formation of homogeneous organic–inorganic hybrid xerogel [24]. Additionally, the nanosize (<0.1 µm) of the silicon titanium oxide particles can match the dimension of pore network of the limestone. On the other hand, the low durability of H_{NST} treatment can be attributed to the photocatalytic oxidation (of the organic radicals) and thermal degradation of the SiO₂-TiO₂ composite, which can weaken the adhesion and thus, durability of the coating [38].

Concerning the drying index, the hydrophobic products induced an increase of the DI on limestone specimens, with higher variation in the case of the H_{Sil} and H_{Sila/Sil} treatments. After aging, H_{Sila/Sil} significantly increase the DI of the treated limestone specimens, whereas H_{Sil} and H_{NST} maintain values similar to unaged specimens. Greater variations are observed in mortar specimens; in fact, the H_{NST} treatment induces an increase of the DI, and a drastic decrease is observed after artificial aging, indicating the probable degradation of the H_{NST} treatment. On the other hand, the H_{Sila/Sil} and H_{Sil} treatments decrease the DI on mortar specimens, with a lower decrease of the latter after artificial aging compared with the H_{NST} treatment. As reported in other works [46], the silane/siloxanes products can modify the pore network of the treated material by increasing the volume of capillary pores, probably also due to an air entraining effect of liquid siloxane. This feature can justify the improved resistance to freeze-thaw cycles, and thus, durability of H_{Sila/Sil} and H_{Sil} treatments compared to H_{NST}.

Furthermore, the difference in the moisture transport properties of treated limestone and mortar can be attributed also to the higher roughness of the mortar, compared to flatter surface of the limestone, which accounts for better adhesion of both fissured and crack free SiO₂-TiO₂ films to the substrate [37].

All treatments induce an increase of the μ in limestone specimens. More specifically, specimens treated with H_{Sila/Sil} and H_{Sil} show the highest μ increase, which significantly decreases after artificial aging in the case of the H_{NST} treatment. The H_{NST} treatment shows a lower μ after artificial aging compared with unaged specimens. Considering the mortar specimens, it can be concluded that μ variation is extremely low with all treatments, both before and after artificial aging. The H_{Sila/Sil} is the only treatment which induced a slight increase of the μ after artificial aging.

Ultimately, it would be expectable that a substrate with higher DI would have also a higher μ (i.e., lower WVP). For treated limestone specimens this trend is confirmed; however, specimens treated with H_{Sila/Sil} have a higher μ /DI ratio (even after artificial aging) compared to the other treatments. A different behavior is observed with treated mortar specimens: Aged and unaged specimens with H_{NST} treatment show the trend mentioned above, whereas unaged H_{Sil} treatment and aged H_{Sila/Sil} treatment show a DI decrease and a μ increase.

5. Conclusions

In this paper, the effectiveness and durability of three commercially available hydrophobic products (a silane and titanium dioxides-based nanostructured dispersion—H_{NST}; a silane/oligomeric siloxane—H_{Sila/Sil}; and a siloxane—H_{Sil}) when applied to a Moleanos limestone and on a cement-based mortar, were analyzed. The alteration of the moisture transport properties (water absorption by

capillarity and under low pressure, drying kinetics and water vapor permeability) of the treated substrates, prior to and after artificial aging tests, was evaluated.

Results show that the effectiveness and durability of the water-repellent treatment is influenced both by the type of hydrophobic product and by the treated substrate.

Although the products were applied at different concentrations, following the recommendations of the producers, all treatments induce a significant decrease of the values of the capillary water absorption and water absorption under low pressure on the mortar specimens. A lower decrease was observed in the limestone specimens. This difference is attributed to the higher open porosity of the mortar specimens compared to limestone specimens, thus allowing a deeper penetration of the hydrophobic products, which increases the water-repellency of the treated mortar. After artificial aging, all hydrophobic treatments show a significant durability to the type and duration of the artificial aging cycles considered in this work, maintaining a reasonably low water absorption in both mortar and limestone specimens, when compared to untreated specimens. The H_{NST} treatment shows a slightly greater loss of efficacy in terms of water capillary absorption and water vapor permeability after artificial aging, mostly when applied on limestone. Therefore, it can be considered less durable.

The treatments induce also a variation of the drying index, which increases with all treatments on limestone specimens (even after artificial drying) and a general decrease on mortar specimens, except for the H_{NST} treatment before aging, which slightly increases the DI. On the other hand, the H_{NST} treatment shows a lower drying index after artificial aging.

$H_{Si1a/Si1}$ and H_{Si1} treatments significantly reduce the water vapor permeability of limestone specimens, whereas the H_{NST} treatment induces a smaller decrease, with values similar to those of untreated specimens after artificial aging. The WVP of the treated mortar specimens was not significantly affected by the hydrophobic treatments, even after aging tests.

These observations confirm that the hydrophobic products are generally more effective and durable on mortar specimens, rather than on low-porosity limestone, as in the case of the studied Moleanos limestone.

When pondering the variation of all the moisture transport properties, the hydrophobic product based on siloxane (H_{Si1}) has the best performance on cement-based mortar; in fact, the molecular structure of siloxanes matches to the higher porosity of this substrate. On the other hand, although it has a lower durability compared to the other treatments, H_{NST} has the best performance when applied on Moleanos limestone, with a significant decrease of the capillary water absorption and a low variation of the drying index and of the WVP. This behavior can result from the combination of the low porosity and micro-sized pores of the stone with the surface deposition of a nanostructured layer. Additionally, the presence of TiO_2 confers antibacterial activity against the microorganism growth and pollutant absorption.

The $H_{Si1a/Si1}$ treatment significantly decreases its water-repellent properties. However, it hinders the drying process and the breathability of the substrates, even after artificial aging. Thus, based on the results of this study, its use is not recommended in either limestone or mortar.

Further tests (e.g., optimization of the protocol; artificial aging cycles with UV light, pollutants and/or biological colonization; FTIR analysis of the hydrophobic products; morphological analysis by SEM-EDS; contact angle measurements of the treated substrates, among others) are ongoing to correlate the effect of the physical-chemical aging on the effectiveness of hydrophobic products, and ultimately, to verify the durability to more prolonged weathering action (from lab to real natural scale tests) of the hydrophobic products.

Author Contributions: Conceptualization, G.B.; Methodology, I.F.-C. and R.V.; Investigation, C.E.; Writing—Original draft preparation, G.B.; Writing—Review and editing, I.F.-C. and R.V.; Supervision, I.F.-C.; Project administration, I.F.-C. All authors have read and agreed to the published version of the manuscript.

Funding: This research was funded by Portuguese Foundation for Science and Technology (FCT), grant number PTDC/ECI-EGC/30681/2017 (WGB_Shield – Shielding building' facades on cities revitalization. Triple resistance for water, graffiti and biocolonization of external thermal insulation systems).

Acknowledgments: The authors acknowledge the companies CIN, Saint-Gobain Weber and NanoPhos for the supply of the hydrophobic products.

Conflicts of Interest: The authors declare no conflict of interest.

References

1. Ferreira Pinto, A.; Delgado Rodrigues, J. Assessment of durability of water repellents by means of exposure testes. In *9th International Congress on Deterioration and Conservation of Stone*; Fassina, V., Ed.; Elsevier: Amsterdam, The Netherlands, 2000; pp. 273–285.
2. Roos, M.; König, F.; Stadtmüller, S.; Weyershausen, B. Evolution of silicone based water repellents for modern building protection. In *5th International Conference on Water Repellent Treatment of Building Materials—Hydrophobe V*; Aedificatio Publishers: Brussels, Belgium, 2008; pp. 3–16.
3. Medeiros, M. Contribuição ao Estudo da Durabilidade de Concretos com Proteção Superficial Frente à ação de íons Cloretos. Ph.D. Thesis, Polytechnic School of the University of São Paulo, São Paulo, Brasil, 2008.
4. Jerman, M.; Černý, R. Effect of moisture content on heat and moisture transport and storage properties of thermal insulation materials. *Energ. Build.* **2012**, *53*, 39–46. [[CrossRef](#)]
5. Pavlík, Z.; Žumár, J.; Medved, I.; Černý, R. Water vapor adsorption in porous building materials: Experimental measurement and theoretical analysis. *Transp. Porous Med.* **2012**, *91*, 939–954. [[CrossRef](#)]
6. Lepech, M.; Li, V. Water permeability of engineered cementitious composites. *Cem. Concr. Comp.* **2009**, *31*, 744–753. [[CrossRef](#)]
7. Silva, L.; Flores-Colen, I.; Vieira, N.; Timmons, A.B.; Sequeira, P. Durability of ETICS and Premixed One-Coat Renders in Natural Exposure Conditions. In *New Approaches to Building Pathology and Durability; Building Pathology and Rehabilitation*; Delgado, J.M.P.Q., Ed.; Springer: Singapore, 2016; Volume 6, pp. 131–158.
8. De Vries, J.; Polder, R. Hydrophobic treatment of concrete. *Constr. Build. Mater.* **1997**, *11*, 259–265. [[CrossRef](#)]
9. Maranhão, F.; Loh, K. *The Use of Hydrophobic Products in Porous Building Materials*; Técnica Edition: São Paulo, Brazil, 2010; p. 155.
10. Ahmad, D.; van den Boogaert, I.; Miller, J.; Presswell, R.; Jouha, H. Hydrophilic and hydrophobic materials and their applications. *Energy Sources Part A* **2018**, *40*, 2686–2725. [[CrossRef](#)]
11. Edwards, P. Preservation for the Future: The need for waterproofing structures above and below ground. *J. Protect. Coat. Linings* **2002**, *7*, 42–46.
12. Finzel, W.; Vincent, H. *Silicones in Coatings. Federation Series on Coatings Technology*; Federation of Societies for Coatings Technology: Philadelphia, PA, USA, 1996.
13. Selley, D. Chemical Considerations for Making Low-VOC Silicon-Based Water Repellents. *J. Coat. Technol. Res.* **2010**, *7*, 26–35.
14. Charola, A. Water repellents and other “protective” treatments: A critical review. In *3rd International Conference on Surface Technology with Water Repellents Agents—Hydrophobe III*; Aedificatio Publishers: Hannover, Germany, 2001; pp. 3–20.
15. Raupach, M.; Buttner, T. Hydrophobic treatments on concrete. Evaluation of the durability and non-destructive testing. In *2nd International Conference on Concrete Repair, Rehabilitation and Retrofitting II*; Alexander, M.G., Beushausen, H.D., Dehn, F., Moyo, P., Eds.; CRC Press: Cape Town, South Africa, 2008; pp. 907–913.
16. Justo, J.; Castro, J.; Cicero, S. Notch effect and fracture load predictions of rock beams at different temperatures using the Theory of Critical Distances. *Int. J. Rock Mech. Min.* **2020**, *125*, 104–161. [[CrossRef](#)]
17. Moura, A.; Flores-Colen, I.; de Brito, J. Study of the effect of three anti-graffiti products on the physical properties of different substrates. *Constr. Build. Mater.* **2016**, *107*, 157–164. [[CrossRef](#)]
18. CEN—European Committee for Standardization. *Methods of Test for Mortar for Masonry—Part 2: Bulk Sampling of Mortars and Preparation of Test Mortars*; EN 1015-2; CEN: Brussels, Belgium, 2006.
19. Esteves, C.; Ahmed, H.; Flores-Colen, I. The influence of hydrophobic protection on building exterior claddings. *J. Coat. Technol. Res.* **2019**, *16*, 1379–1388. [[CrossRef](#)]
20. Rutter, T.; Hutton-Prager, B. Investigation of hydrophobic coatings on cellulose-fiber substrates with in-situ polymerization of silane/siloxane mixtures. *Int. J. Adhes. Adhes.* **2018**, *86*, 13–21. [[CrossRef](#)]

21. Qiao, B.; Liang, Y.; Wang, T.J.; Jiang, Y. Surface modification to produce hydrophobic nano-silica particles using sodium dodecyl sulfate as a modifier. *Appl. Surf. Sci.* **2016**, *364*, 103–109. [[CrossRef](#)]
22. Yu, K.; Liang, Y.; Ma, G.; Yang, L.; Wang, T.Y. Coupling of synthesis and modification to produce hydrophobic or functionalized nano-silica particles. *Colloid Surf. A* **2019**, *574*, 122–130. [[CrossRef](#)]
23. Kapridaki, C.; Maravelaki-Kalaitzaki, P. TiO₂–SiO₂–PDMS nano-composite hydrophobic coating with self-cleaning properties for marble protection. *Prog. Org. Coat.* **2013**, *76*, 400–410. [[CrossRef](#)]
24. Alfieri, I.; Lorenzi, A.; Ranzenigo, A.; Lazzarini, L.; Predieri, G.; Lottici, P.P. Synthesis and characterization of photocatalytic hydrophobic hybrid TiO₂–SiO₂ coatings for building applications. *Build. Environ.* **2017**, *111*, 72–79. [[CrossRef](#)]
25. Truppi, A.; Luna, M.; Petronella, F.; Falcicchio, A.; Giannini, C.; Comparelli, R.; Mosquera, M.J. Photocatalytic activity of TiO₂/AuNRs–SiO₂ nanocomposites applied to building materials. *Coatings* **2018**, *8*, 296. [[CrossRef](#)]
26. CEN—European Committee for Standardization. *Methods of Test for Mortar for Masonry—Part 18: Determination of Water Absorption Coefficient due to Capillary Action of Hardened Mortar*; EN 1015-18; CEN: Brussels, Belgium, 2002.
27. RILEM. Water Absorption under Low Pressure, Pipe Method, Test No 11.4. In *Recommandations Provisoires*; RILEM TC 25-PEM; RILEM Publications SARL: Paris, France, 1980; pp. 201–202.
28. RILEM. *Evaporation Curve, Test No 11.5*; *Recommandations Provisoires*; RILEM TC 25-PEM; RILEM Publications SARL: Paris, France, 1980; pp. 205–207.
29. *NORMAL 29/88—Misure dell'Indice di Asciugamento (Drying Index), Alterazioni dei Materiali Lapidei e Trattamenti Conservativi—Proposte per l'unificazione dei Metodi Sperimentali di Studio e Controllo*; ICR-CNR: Rome, Italy, 1988.
30. CEN—European Committee for Standardization, *Methods of Test for Mortar for Masonry—Part 19: Determination of Water Vapour Permeability of Hardened Rendering and Plastering Mortars*; EN 1015-19; CEN: Brussels, Belgium, 2008.
31. Velosa, A.; Veiga, M.R. Development of Artificial Ageing Tests for Renders—Application to Conservation Mortars. In *7th International Masonry Conference—7IMC*; Thompson, G., Ed.; International Masonry Society: London, UK, 2006.
32. Veiga, M.R.; Santos Silva, A. *Long-term Performance and Durability of Masonry Structures Degradation Mechanisms, Health Monitoring and Service Life Design, Chapter 6—Mortars*; Woodhead Publishing Series in Civil and Structural, Engineering; Ghiassi, B., Lourenço, P., Eds.; Elsevier: Amsterdam, The Netherlands, 2019; pp. 169–208.
33. CEN—European Committee for Standardization, *Methods of test for Mortar for Masonry—Part 21: Determination of the Compatibility of One-Coat Rendering Mortars with Substrates*; EN 1015-21; CEN: Brussels, Belgium, 2002.
34. Pascoal, P.; Borsoi, G.; Veiga, R.; Faria, P.; Santos Silva, A. Consolidation and chromatic reintegration of historical renders with lime-based pozzolanic products. *Stud. Conser.* **2015**, *60*, 321–332.
35. Maia, J.; Ramos, N.M.M.; Veiga, R. Assessment of test methods for the durability of thermal mortars exposure to freezing. *Mater. Struct.* **2019**, *52*, 112. [[CrossRef](#)]
36. Thomson, M.L.; Lindqvist, J.E.; Elsen, J.; Groot, C.J.W.P. Porosity of historic mortars. In *Characterisation of Old Mortars with Respect to Their Repair—Final Report of RILEM TC 167-COM*; Groot, C., Ashall, G., Hughes, J., Eds.; RILEM Publications SARL: Paris, France, 2004; pp. 77–106.
37. Li, Z.; Liu, L.; Yan, S.; Zhang, M.; Xia, J.; Xie, Y. Effect of freeze-thaw cycles on mechanical and porosity properties of recycled construction waste mixtures. *Constr. Build. Mater.* **2019**, *210*, 347–363. [[CrossRef](#)]
38. Calia, A.; Lettieri, M.; Masieri, M. Durability assessment of nanostructured TiO₂ coatings applied on limestones to enhance building surface with self-cleaning ability. *Build. Environ.* **2016**, *110*, 1–10. [[CrossRef](#)]
39. Nogueira, R.; Ferreira Pinto, A.P.; Gomes, A. Artificial ageing by salt crystallization: Test protocol and salt distribution patterns in lime-based rendering mortars. *J. Cult. Herit.* **2020**. [[CrossRef](#)]
40. Hunt, A.; Ewing, R. *Percolation Theory for Flow in Porous Media*, 2nd ed.; Lect. Notes in Phys.; Springer: Heidelberg, Germany, 2008; p. 771.
41. Santos, A.R.; Veiga, M.R.; Santos Silva, A.; de Brito, J. Tensile bond strength of lime-based mortars: The role of the microstructure on their performance assessed by a new non-standard test method. *J. Build. Eng.* **2020**, *29*, 101136. [[CrossRef](#)]
42. Hall, C.; Hoff, W.D. *Water Transport in Brick, Stone and Concrete*; Spon Press, Taylor & Francis Group: New York, NY, USA, 2012.

43. Tsakalofa, A.; Manoudisb, P.; Karapanagiotisc, I.; Chryssoulakisc, I.; Panayiotoub, C. Assessment of synthetic polymeric coatings for the protection and preservation of stone monuments. *J. Cult. Herit.* **2007**, *8*, 69–72. [[CrossRef](#)]
44. Lucquiaud, V.; Courard, L.; Gérard, O.; Michel, F.; Handy, M. Evaluation of the durability of hydrophobic treatments on concrete architectural heritage. *Restor. Build. Monum.* **2015**, *20*, 395–404.
45. Guo, T.; Weng, X. Evaluation of the freeze-thaw durability of surface-treated airport pavement concrete under adverse conditions. *Constr. Build. Mater.* **2019**, *206*, 519–530. [[CrossRef](#)]
46. Falchi, L.; Zendri, E.; Müller, U.; Fontana, P. The influence of water-repellent admixtures on the behaviour and the effectiveness of Portland limestone cement mortars. *Cem. Concr. Comp.* **2015**, *59*, 107–118. [[CrossRef](#)]



© 2020 by the authors. Licensee MDPI, Basel, Switzerland. This article is an open access article distributed under the terms and conditions of the Creative Commons Attribution (CC BY) license (<http://creativecommons.org/licenses/by/4.0/>).